Asian Journal of Chemistry; Vol. 25, No. 10 (2013), 5732-5734

ASIAN JOURNAL OF CHEMISTRY

http://dx.doi.org/10.14233/ajchem.2013.OH77

Preparation and Characterization of the Conductive $Co_{(1-x)}Ni_xFe_2O_4$/Polypyrrole Microsphere Composites†

CHANGSEN ZHANG*, LEI YANG, QISHENG WU and JUHUA LUO

School of Materials Engineering, Yancheng Institute of Technology, Yancheng 224051, P.R. China

*Corresponding author: Fax: +86 515 88298249; E-mail: zcs@ycit.cn

AJC-13319

$Co_{(1-x)}Ni_xFe_2O_4$ nanoparticles were synthesized by a sol-gel method and then the core-shell structure $Co_{(1-x)}Ni_xFe_2O_4$/polypyrrole nanocomposites, where the core was $Co_{(1-x)}Ni_xFe_2O_4$ and the shell was polypyrrole, were prepared by *in situ* polymerization. Phase composition, microstructure and magnetic properties of the samples were investigated by Fourier transform spectrometer, X-ray diffraction diffractometer, scanning electron microscope and superconductor quantum interference device. The results indicate that the average sizes of $Co_{(1-x)}Ni_xFe_2O_4$/polypyrrole nanocomposites are about 100 nm. The saturation magnetization of the pure $Co_{(1-x)}Ni_xFe_2O_4$ nanoparticles are 52.3 emu/g, but $Co_{(1-x)}Ni_xFe_2O_4$/polypyrrole composites are 37.36 emu/g. Both $Co_{(1-x)}NixFe_2O_4$ and $Co_{(1-x)}Ni_xFe_2O_4$/PPy showed superparamagnetism.

Key Words: Core-shell structure, $Co_{(1-x)}Ni_xFe_2O_4$, Conductive polypyrrole, Magnetic property.

INTRODUCTION

Conducting polymer based composites with electrical, magnetic and optical properties have attracted attention in various fields such as electromagnetic interference shielding, rechargeable batteries, corrosion equipment and microwave absorbing materials, *etc*. Spinal ferrites and hexagonal ferrites are widely studied because of their interesting magnetic properties as well as extensive potential applications in biomedical, magnetic recording media, soft magnetic materials and absorbing materials. To improve the properties of polymers and ferrites and thus enlarge their application, conducting polymer and ferrite were prepared usually composites[1-6], such as core-shell structure ferrite/polymer nanocomposites.

In the past decade, several organic magnetic composites with both electrical and magnetic properties were studied widely. Saafan *et al.*[7] studied DC conductivity and relative magnetic permeability of nanoparticle $NiZnFe_2O_4$/polypyrrole composites. Xie *et al.*[8] reported synthesis and characterization of La/Nd-doped barium-ferrite/polypyrrole nanocomposites. Li *et al.*[9] reported fabrication and electromagnetic characteristics of microwave absorbers containing polypyrrole and carbonyl iron composite. This study involves to develop microwave absorbers using both dielectric and magnetic lossy materials. Polypyrrole is used as dielectric lossy materials and carbonyl iron particles is used as magnetic lossy materials. Polypyrrole (PPY) powders are prepared by in situ polymerization method. Zhang *et al.*[10] studied α-Fe_2O_3/PPy/Ag functional hybrid nanomaterials with core/shell structure. Synthesis, characterization and catalytic activity show nanocomposites composed of hematite, polypyrrole and silver. A surface redox between polypyrrole and silver salt was used. The nanocomposites were with typical core/shell structure. Nanocomposites showed good electrochemical property.

In the present work, shell-core-structured $Co_{(1-x)}Ni_xFe_2O_4$/PPY nanocomposites were prepared by *in situ* polymerization in hydrochloric acid solution. Phase composition, microstructure and magnetic properties of $Co_{(1-x)}Ni_xFe_2O_4$/PPY were investigated by Fourier transform spectrometer (FT-IR), X-ray diffraction diffractometer (XRD), scanning electron microscope (SEM), differential thermal analysis (TG-DSC) and superconductor quantum interference device (SQUID).

EXPERIMENTAL

Sample preparation: $CoCl_2 \cdot 6H_2O$ (analytical grade), $NiSO_4 \cdot 6H_2O$ (analytical grade), citric acid (analytical grade) and $FeCl_3$ (chemical grade) were used as raw materials. The molar ratio of Co^{2+}, Ni^{2+}, Fe^{3+} and citric acid were controlled at 0.5:0.5:1:1. Stoichiometric amount of $CoCl_2 \cdot 6H_2O$, $NiSO_4 \cdot 6H_2O$, $FeCl_3$ and citric acid were dissolved in 50 mL distilled water, then the solution was stirred 5 h continuously at around 80 ºC in water bath until the gel was formed. Then the obtained

†Presented to the 6th China-Korea International Conference on Multi-functional Materials and Application, 22-24 November 2012, Daejeon, Korea

gel was dried in an oven at 80 ºC for 24 h. Finally the dried gel was put in Muffle furnace at 1000 ºC for 2 h, the final powders was obtained.

1.4 mL pyrrole (analytical grade) and 0.27 g $Co_{(1-x)}Ni_xFe_2O_4$ nanoparticles were mixed in 150 mL 1 mol/L hydrochloric acid solution with ultrasonic dispersion for 30 min. Then an aqueous solution of $(NH_4)_2S_2O_8$ (ammonium persulfate, 6.25 g was dissolved in 50 mL 1 mol/L hydrochloric acid solution) slowly added dropwise into the above reactant mixtures with stirring for 24 h at around 0 ºC under an ice-water bath. The obtained dark yellow solids were filtered, washed thoroughly with ethanol and distilled water, respectively and dried at 80 ºC for 24 h in vacuum. The target composite was prepared.

Analysis and characterization: The morphology and microstructure of PPy, $Co_{(1-x)}NixFe_2O_4$ and $Co_{(1-x)}Ni_xFe_2O_4$/PPy particles were characterized by scanning electron microscope (SEM, Fei Quanta-200, America). Chemical bonds structure was analyzed by Fourier Transform Infrared (FT-IR, Niocelt NEXUS-670, America). Phase structure of samples were characterized by X-ray diffraction (Philps-PW3040/60) with CuK_α radiation ($\lambda = 0.15406$ nm), scan rate for 5º/min. Magnetic properties were analysized by superconducting quantum interference device magnetic measurement system (SQUID, MPMS-XL-7, American).

RESULTS AND DISCUSSION

FT-IR spectral analysis: Fig. 1 shows the FT-IR spectra of polypyrrole(a) and $Co_{(1-x)}Ni_xFe_2O_4$/PPY(b). In Fig. 1 (a), the peaks at 3439 cm^{-1} is attributed to the characteristic N-H stretching vibration band[11] and the peak at 1548 cm^{-1} is assigned to C-C and C=C stretching vibration combination band. The peak of 1461 cm^{-1} is attributed to C-C stretching modes[12], 1294 cm^{-1} and 1043 cm^{-1} are attributed to the in-plane deformation vibration band of C-H[13]. The peak of 1189 cm^{-1} is attributed to C-N stretching vibrations. The peaks of 916 cm^{-1} and 788 cm^{-1} are attributed to out of plane ring deformation vibration of C-H and 614 cm^{-1} is attributed to out of plane ring deformation vibration of C-C[7]. In addition, the peak at 1639 cm^{-1} may be due to the PPy oxidized over. In Fig. 1 (b) and (a) are very similar, (b) shows not only the characteristic peaks of the PPy but also the peaks of stretching vibration attributed to Fe-O in spinel structure of $Co_{(1-x)}Ni_xFe_2O_4$ at 505 cm^{-1} and 434 cm^{-1}. Fig. 1(b) and (a) are very similar and (b) at 3449, 1631, 1305, 1190, 1046, 792 and 619 cm^{-1} are attributed to corresponding peaks. These peaks have occurred different degree of red shift due to the interactions between the $Co_{(1-x)}Ni_xFe_2O_4$ and the PPy, it weakens the N-H, C-H and the C=C bond interactions. In addition, the peaks at 505 cm^{-1} and 434 cm^{-1} is the Fe-O of the spinel structure of $Co_{(1-x)}Ni_xFe_2O_4$[8].

The IR spectra of $Co_{(1-x)}Ni_xFe_2O_4$/PPy composites are almost identical to that of polypyrrole. But to some extent, the spectra of PPy in composites is slightly red shift. It indicates that the ferrite particles are well encapsulated by PPy chains and there are some interactions between the $Co_{(1-x)}Ni_xFe_2O_4$ and the PPy, it weakens the N-H, C-H and the C=C bond interactions. These results also show that the compositions of the composites are PPy and $Co_{(1-x)}Ni_xFe_2O_4$.

X-ray analysis: Phase investigation of the crystallized products is performed by XRD and the patterns of polypyrrole,

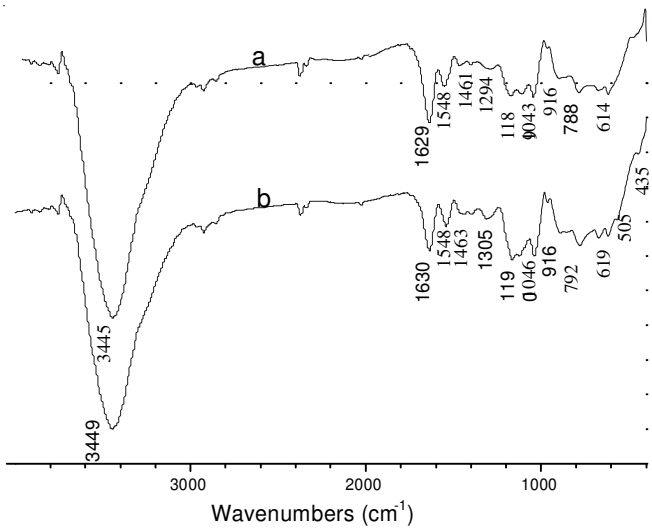

Fig. 1. FT-IR spectra of PPy (a) and $Co_{(1-x)}Ni_xFe_2O_4$/PPy nanocomposites (b)

$Co_{(1-x)}Ni_xFe_2O_4$ and $Co_{(1-x)}Ni_xFe_2O_4$/PPy composites are presented in Fig. 2. In Fig. 2a, it can be seen that the near 2θ value of 25º appear the diffuse width diffraction peak of the PPy of amorphous structure. In Fig. 2b, it can be seen that some peaks being well scored with the date of JCPDS card 52-278 for $Co_{0.5}Ni_{0.5}Fe_2O_4$ ferrite. The peaks at around 18.42, 30.29, 35.68, 37.33, 43.36, 53.82, 57.37 and 63.00 are well corresponded to the crystal planes of spinel ferrite (111), (220), (311), (222), (400), (422), (511) and (440), respectively. In Fig. 2c, it can be seen some features diffraction peaks of $Co_{0.5}Ni_{0.5}Fe_2O_4$ ferrite, but these diffraction intensity of peak obviously less than pure $Co_{0.5}Ni_{0.5}Fe_2O_4$. It should be noted that the amorphous nature of the nanocomposites increases. This can be attributed to the presence of a layer of PPy in the composites. The presence of broad diffraction pattern around 2θ value of 25º indicates planar configuration of PPy due to the densely packed phenyl rings. No other material is found in XRD patterns. It indicates that $Co_{(1-x)}Ni_xFe_2O_4$ and PPy do not produce chemical reaction. $Co_{(1-x)}Ni_xFe_2O_4$ nanoparticles is confirmed in core position as the polymerization of pyrrole monomer.

This result also indicates that the composites contain $Co_{(1-x)}Ni_xFe_2O_4$ ferrite and PPy. When the grain size is less than

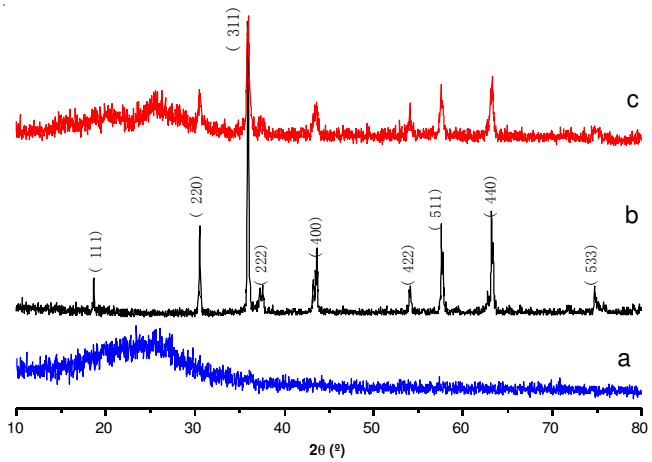

Fig. 2. X-ray diffraction patterns of the PPy (a), $Co_{(1-x)}Ni_xFe_2O_4$ (b) and $Co_{(1-x)}Ni_xFe_2O_4$/PPY nanocomposites (c)

100 nm, an effective method to calculate the grain size is the X-ray diffraction line half width method. According to Scherrer formula (1), where λ is the X-ray wavelength and *k* is the shape factor depends on several factors including the Miller index of the reflecting plane and shape of the crystal. If the shape is unknown, *k* is often assigned a value of 0.89. D is the average diameter of the crystal in angstroms, θ is the Bragg angle in degree and β is the line broadening measured by half-height in radium. By calculating, the average size of nanograin $Co_{(1-x)}Ni_xFe_2O_4$ is 67.0 nm.

$$\beta = \frac{k\lambda}{D\cos\theta} \quad (1)$$

Morphology analysis: The SEM of $Co_{(1-x)}Ni_xFe_2O_4$ (a) and (b); HCl-PPY (c) and $Co_{(1-x)}Ni_xFe_2O_4$/PPy (d) composites are shown in Fig. 3. It can be seen that the morphology of the PPy and $Co_{(1-x)}Ni_xFe_2O_4$/PPy composite particles are basically globular, $Co_{(1-x)}Ni_xFe_2O_4$ particles are the cubic tapered morphology. The results show that the $Co_{(1-x)}Ni_xFe_2O_4$/PPy composites are core-shell nanoparticles where the core is $Co_{(1-x)}Ni_xFe_2O_4$ and the shell is PPy, which is in accordance with the results obtained by XRD analysis.

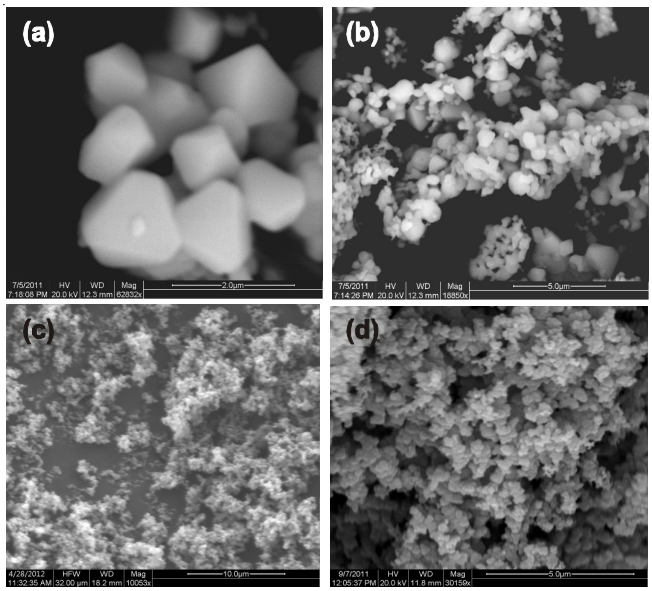

Fig. 3. SEM micrographs of the $Co_{(1-x)}Ni_xFe_2O_4$ (a), (b); HCl-PPY (c); $Co_{(1-x)}Ni_xFe_2O_4$/PPy nanocomposites (d)

Magnetic properties: Hysteresis loops of the $Co_{(1-x)}Ni_xFe_2O_4$ nanoparticles and $Co_{(1-x)}Ni_xFe_2O_4$/PPy nanocomposites are shown in Fig. 4. From Fig.4, the saturation magnetization (Ms) of pure $Co_{(1-x)}Ni_xFe_2O_4$ is 52.3 emu/g at 300 K, which is obviously higher than that of $Co_{(1-x)}Ni_xFe_2O_4$/PPy nanocomposites (37.3 emu/g). This may be attributed to the lower $Co_{(1-x)}Ni_xFe_2O_4$ content (15 wt %), smaller size and their uneven distribution of $Co_{(1-x)}Ni_xFe_2O_4$ nanoparticles in the final microsphere composites.

In addition, when the magnetic field intensity decreases to zero, the magnetization decreases from the plateau value to nealy zero, suggesting that the coercive force is very low. The hysteresis loop present superparamagnetic of nanoparticles and this property can prevent the polymer magnetic composite microspheres from aggregation and enable them to redisperse rapidly when the magnetic field was removed.

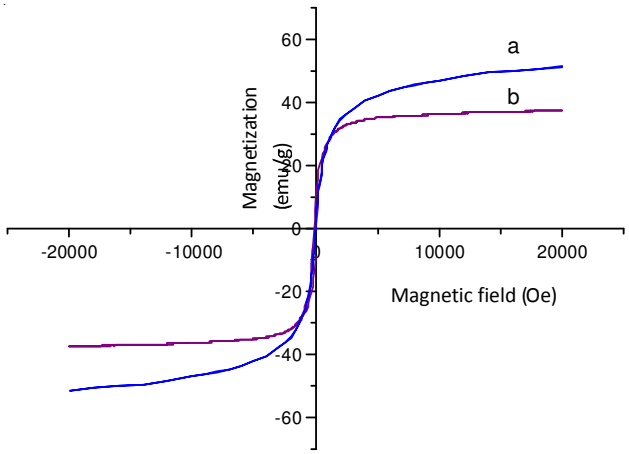

Fig. 4. Hysteresis loops of $Co_{(1-x)}Ni_xFe_2O_4$ nanoparticles at 300K (a) and $Co_{(1-x)}Ni_xFe_2O_4$/PPy nanocomposites at 300 K (b)

Conclusion

$Co_{(1-x)}Ni_xFe_2O_4$ nanoparticles were synthesized by a sol-gel method. The core-shell structure core-shell structure $Co_{(1-x)}Ni_xFe_2O_4$/PPy nanocomposites were prepared successfully by in situ polymerization method and characterized by Fourier transform spectrometer, X-ray diffraction diffractometer, Scanning electron microscope and Superconductor quantum interference device. They have intermolecular interactions between the PPY and $Co_{(1-x)}Ni_xFe_2O_4$ ferrite in the composites. The average sizes of the PPy and $Co_{(1-x)}Ni_xFe_2O_4$ nanocomposites are about 100 nm. In addition, the Ms of the $Co_{(1-x)}Ni_xFe_2O_4$/PPy (37.36 emu/g) nanocomposites are lower than that of the pure $Co_{(1-x)}Ni_xFe_2O_4$ (52.3 emu/g). Both $Co_{(1-x)}Ni_xFe_2O_4$ and $Co_{(1-x)}Ni_xFe_2O_4$/PPy showed superparamagnetism.

ACKNOWLEDGEMENTS

The work was supported in part by Jiangsu Province College Science Major Basic Research project (10KJA430054).

REFERENCES

1. J. Stejskal, M. Trchová, J. Brodinová, P. Kalenda, S.V. Fedorova, J. Prokeš and J. Zemek, *J. Colloid Interf. Sci.*, **298**, 87 (2006).
2. N.E. Kazantseva, Yu.I. Bespyatykh, I. Sapurina, J. Stejskal, J. Vilcáková and P. Sáha, *J. Magnet. Magnet. Mater.*, **301**, 155 (2006).
3. V. Babayan, N.E. Kazantseva, R. Moucka, I. Sapurina, Yu.M. Spivak and V.A. Moshnikov, *J. Magnet. Magnet. Mater.*, **324**, 161 2012 (2012).
4. L.-J. Cao, Q.-H. Zhou, L. Gu, H.-X. Shen, Q.-H. Li, P. Lan and Y. Fang, *Trans. Nonferrous Met. Soc. China*, **22**, 360 (2012).
5. N.E. Kazantseva, J. Vilcáková, V. Kresálek, P. Sáha, I. Sapurina and J. Stejskal, *J. Magnet. Magnet. Mater.*, **269**, 30 (2004).
6. C.S. Zhang and L. Yang, *J. Magnet. Magnet. Mater.*, **324**, 1469 (2012).
7. S.A. Saafan, T.M. Meaz and E.H. El-Ghazzawy, *J. Magnet. Magnet. Mater.*, **323**, 1517 (2011).
8. Y. Xie, X. Hong, Y. Gao, M. Li, J. Liu, J. Wang and J. Lu, *Synth. Metals*, **162**, 677 (2012).
9. D.-A. Li, H.-B. Wang, J.-M. Zhao and X.L. Yang, *Mater. Chem. Phys.*, **130**, 437 (2011).
10. X. Zhang, W.-X. Zhi, B. Yan and X.-X. Xu, *Powder Technol.*, **221**, 177 (2012).
11. H.C. Kand and K.E. Geckeler, *Polymer*, **41**, 6931 (2000).
12. J. Liu and M. Wan, *J. Polym. Sci. A*, **38**, 2734 (2000).
13. L.J. Bellamy, The Infrared Spectra of Complex Moleeules, Chapman & Hall, London, edn. 2, vol. 2 (1980).